Orissa Journal of Physics
ISSN 0974-8208

Vol. 31, No.2
August 2024
pp. 154-167

Effects of Spacetime Curvature on the Gravitational Redshift in Dark Matter-admixed Quarkyonic Stars

JEET AMRIT PATTNAIK[1], D. DEY[2], M. BHUYAN[2,*] , R. N. PANDA[1] , and S. K. PATRA[1]

[1]*Department of Physics, Siksha ' O ' Anusandhan Deemed to be University, Bhubaneswar -751030, India*
[2]*Institute of Physics, Sachivalaya Marg, Bhubaneswar-751005, Odisha, India*

**Corresponding author. E-mail: mrutunjaya.b@iopb.res.in*

Received xx.xx.25, Accepted xx.xx.25

Abstract. We investigate the effects of spacetime curvature on the gravitational redshift in dark matter-admixed quarkyonic stars using the effective relativistic mean-field (E-RMF) approach. These compact objects, known as neutron stars, are characterized by a mixture of quarkyonic matter and fermionic dark matter (DM) and exhibit distinct gravitational properties because of the combined stiffening and softening of the equation of state. We analyze the Kretschmann scalar curvature ratio $(K(R)/K_{\odot})$ to obtain the gravitational redshift at the stellar surface as a function of dark matter content and transition density. Our results show that dark matter significantly enhances the gravitational potential, leading to a stronger redshift near the star's surface. Stars with higher DM Fermi momenta (K_f^{DM}=0.03, 0.04 GeV) exhibit larger curvature ratios compared to purely baryonic stars. These effects provide distinct signatures differentiating dark matter-admixed quarkyonic stars from normal neutron stars.

Keywords: Nuclear matter, Quarkyonic matter, Dark matter, Spacetime curvature, Gravitational redshift

1. Introduction

Neutron stars (NSs) are among the most compact and dense objects in the Universe, distinguished by their exceptionally high core densities and solid crusts. These extraordinary properties allow them to sustain persistent deformations, making them potential sources of gravitational waves (GWs).

The extreme conditions within NSs provide a natural laboratory for testing theories of matter in high-density and strong-gravity environments [1, 2]. Primarily composed of neutrons, NSs also contain smaller proportions of protons and leptons. At higher densities, exotic matter—such as hyperons, meson condensates, or deconfined quarks—becomes possible within their cores. As highlighted in our previous work [3], significant progress has been made in constraining NS properties due to recent observational advancements. Precise mass measurements exceeding and radius constraints from events such as GW170817 [4, 5, 6, 7], together with NICER pulsar X-ray data [8, 9], have imposed stringent limits on EOS. For example, the radius of a canonical NS 1.4 $M_{\odot}$ is now restricted to be below 13.5 km [10, 11]. Furthermore, observations of high-mass pulsars, such as PSR J0952-0607 and J0740+6620, with masses of 2.35 ± 0.17 $M_{\odot}$ and 2.08 ± 0.07 $M_{\odot}$, respectively, offer additional EOS constraints [12, 13]. These findings have helped the development of theoretical models, such as the quarkyonic matter framework, which postulates a transition between nucleonic and quark phases within NS cores. This model envisions quarks as quasi-particles emerging at high densities, significantly influencing the EOS and pressure profiles [14, 3]. In our earlier study [3], we adopted this approach to investigate how dark matter (DM) and quark matter affect the EOS and macroscopic NS properties, exploring the interplay between nucleonic, quark, and DM components.

The inclusion of DM in NS models is partly motivated by the GW190814 event, which involved the merger of a black hole (22.2–24.3 $M_{\odot}$) with a secondary compact object of 2.50–2.67$M_{\odot}$ [15]. This enigmatic secondary object, potentially the most massive NS or the lightest black hole observed, suggests the possible presence of DM within NSs. The extent of DM capture within NSs influences key properties, such as mass, radius, and tidal deformability (Λ) [16, 17, 18, 19, 20, 21, 22, 23, 24, 25, 26, 27, 28, 29]. In this work, we consider non-annihilating weakly interacting massive particles (WIMPs) as the DM candidates, whose inclusion softens the EOS, reducing the NS's mass and radius. Using the Effective Relativistic Mean-Field (E-RMF) theory—a robust framework for modelling dense nuclear matter—we extend the formalism to incorporate both quark matter and DM. This allows us to analyze their combined effects on NS structure. Our study focuses on impact of curvature properties on redshift of quarkyonic NSs with DM, employing the G3 [30] and IOPB-I [31] parameter sets, known for accurately reproducing finite nuclear properties and aligning with observational constraints, including mass, radius, and tidal deformability [30, 31, 3, 32, 33]. Furthermore, the gravitational redshift is a fundamental phenomenon that arises from the intense gravitational field of neutron stars, where emitted radiation experiences a shift towards longer wavelengths as it escapes the star's strong gravity. This redshift directly indicates the compactness of the star, defined as the ratio of its mass to radius, providing crucial insights into the density matter equation of state (EOS). For a neutron star, the redshift is expressed as $z = (1 - 2GM/Rc^2)^{-1/2} - 1$ where G is the gravitational constant, M is the mass of the star, R is its radius, and c is the speed of light. As measured by NICER, observations of redshifted spectral lines from the surface of neutron stars can constrain the star's mass and radius, narrowing down the EOS and play a critical role in energy spectra of the emitted radiation, making it a valuable tool for probing spacetime curvature and the extreme physics governing neutron stars [34, 35]. The geometry of spacetime surrounding NSs offers critical insights into the EOS of dense matter.

Curvature measures, such as the Ricci scalar, Kretschmann scalar, and Ricci and Weyl tensors, describe spacetime warping caused by the star's immense compactness [34, 35]. Mathematically, spacetime curvature is described by the Riemann tensor, which encapsulates tidal forces and deformation. Derived quantities, such as the Kretschmann scalar (curvature magnitude), Ricci tensor (volumetric changes), and Weyl tensor (shape distortions), provide comprehensive curvature metrics [36, 29]. Recent studies, such as those of Eksi et al. [37] and Xiao et al. [35], demonstrate that the symmetry energy has a strong dependence on the curvature in low-mass NSs, decreasing in their higher-mass counterparts. Our recent work [38] also explores the impact of anisotropy on NS surface curvature and provides approximate relationships linking curvature with tidal deformability and moment of inertia.

This paper is structured as follows: Section 2 outlines the theoretical framework, focusing on the E-RMF approach and its extensions for quark matter and DM. Section 3 presents the study's findings, while Section 4 provides concluding remarks.

2. Effective Relativistic Mean Field Approach

The effective relativistic mean-field (E-RMF) formalism is a robust theoretical framework for studying both finite nuclei and infinite nuclear matter (NM) [32, 39, 33, 40]. Its parameters are carefully tuned using a broad range of experimental and empirical data. More than 200 parameter sets have been developed to replicate various experimental and observational results [41, 42, 43, 44, 45, 46, 47, 48, 49, 31, 50]. For this study, we used the E-RMF model, thoroughly detailed in Refs. [29, 51, 52, 53, 54]. The inclusion of leptonic contributions is essential to maintain the stability of neutron stars. Consequently, the energy density $\mathcal{E}_{\rm BM}$ and pressure $P_{\rm BM}$ for a system composed of NM and leptons are derived using stress-energy tensor methods [54],

$$\begin{aligned}
\mathcal{E}_{\rm BM} = & \sum_{i=p,n} \frac{g_s}{(2\pi)^3} \int_0^{k_{f_i}} d^3k \sqrt{k^2 + M_{\rm nucl.}^{*2}} \\
& + n_b g_\omega\, \omega + m_\sigma^2 \sigma^2 \left(\frac{1}{2} + \frac{\kappa_3}{3!} \frac{g_\sigma \sigma}{M_{\rm nucl.}} + \frac{\kappa_4}{4!} \frac{g_\sigma^2 \sigma^2}{M_{\rm nucl.}^2} \right) \\
& - \frac{1}{4!} \zeta_0\, g_\omega^2\, \omega^4 - \frac{1}{2} m_\omega^2\, \omega^2 \left(1 + \eta_1 \frac{g_\sigma \sigma}{M_{\rm nucl.}} + \frac{\eta_2}{2} \frac{g_\sigma^2 \sigma^2}{M_{\rm nucl.}^2} \right) \\
& + \frac{1}{2} (n_n - n_p)\, g_\rho\, \rho - \frac{1}{2} \left(1 + \frac{\eta_\rho g_\sigma \sigma}{M_{\rm nucl.}} \right) m_\rho^2 \\
& - \Lambda_\omega\, g_\rho^2\, g_\omega^2\, \rho^2\, \omega^2 + \frac{1}{2} m_\delta^2\, \delta^2 \\
& + \sum_{j=e,\mu} \frac{g_s}{(2\pi)^3} \int_0^{k_{F_j}} \sqrt{k^2 + m_j^2}\, d^3k, \qquad (1)
\end{aligned}$$

and

$$\begin{aligned}
P_{\rm BM} = & \sum_{i=p,n} \frac{g_s}{3(2\pi)^3} \int_0^{k_{f_i}} d^3k \frac{k^2}{\sqrt{k^2 + M_{\rm nucl.}^{*2}}} \\
& - m_\sigma^2 \sigma^2 \left(\frac{1}{2} + \frac{\kappa_3}{3!} \frac{g_\sigma \sigma}{M_{\rm nucl.}} + \frac{\kappa_4}{4!} \frac{g_\sigma^2 \sigma^2}{M_{\rm nucl.}^2} \right) + \frac{1}{4!} \zeta_0\, g_\omega^2\, \omega^4
\end{aligned}$$

$$+\frac{1}{2}m_\omega^2\omega^2\left(1+\eta_1\frac{g_\sigma\sigma}{M_{\rm nucl.}}+\frac{\eta_2}{2}\frac{g_\sigma^2\sigma^2}{M_{\rm nucl.}^2}\right)$$
$$+\frac{1}{2}\left(1+\frac{\eta_\rho g_\sigma\sigma}{M_{\rm nucl.}}\right)m_\rho^2\rho^2-\frac{1}{2}m_\delta^2\delta^2+\Lambda_\omega g_\rho^2 g_\omega^2\rho^2\omega^2$$
$$+\sum_{j=e,\mu}\frac{g_s}{3(2\pi)^3}\int_0^{k_{F_j}}\frac{k^2}{\sqrt{k^2+m_j^2}}\,d^3k, \quad (2)$$

where, g_s and M denote the spin degeneracy and nucleon mass, while m_σ, m_ω, m_ρ, and m_δ represent the meson masses. The coupling constants g_σ, g_ρ and g_δ correspond to interactions with these mesons. Additional parameters like κ_3, κ_4, ζ_0, η_1, η_2, η_ρ, and Λ_ω describe meson self-interactions and cross-couplings [55, 56, 57, 58, 59, 54, 31].

2.1. Quarkyonic Model

The quarkyonic model, proposed by McLerran and Reddy [60], describes a transition to a phase where nucleons break into quarks at densities far exceeding nuclear saturation density. This transition is marked by a significant pressure increase due to quark population in low-momentum states when baryon density surpasses a critical threshold (transition density). In this phase, quarks occupy low-momentum states, while nucleons dominate near the Fermi surface, with their momenta scaling with the QCD confinement scale, Λ_{cs}. Zhao and Lattimer [14] refined this model by incorporating beta-equilibrium and charge neutrality, along with density-dependent nucleon interactions. They also introduced chemical equilibrium between nucleons and quarks, linking nucleonic ($k_{f_{n,p}}$) and quark ($k_{f_{u,d}}$) Fermi momenta. Nucleons occupy a finite Fermi shell, bounded by lower ($k_{f0_{(n,p)}}$) and upper ($k_{f_{n,p}}$) Fermi momentum limits. Quark Fermi momenta are similarly defined as $k_{f_u}$and k_{f_d}. A detailed analysis of this framework can be found in our recent study [3]. The quarks energy density $\mathcal{E}_{\rm QM}$ and pressure $P_{\rm QM}$ can be expressed as [14, 3],

$$\mathcal{E}_{\rm QM}=\sum_{j=u,d}\frac{g_s N_c}{(2\pi)^3}\int_0^{k_{f_j}}k^2\sqrt{k^2+m_j^2}\,d^3k, \quad (3)$$

and

$$P_{\rm QM}=\mu_u n_u+\mu_d n_d-\epsilon_{QM} \quad (4)$$

2.2. Dark Matter Model

The dark matter Lagrangian density [22, 27, 26, 3] is constructed based on the interaction of DM particles with both nucleons and quarks channelling through Higgs exchange, which is defined as,

$$\mathcal{L}_{\rm DM} = \bar{\chi}\left[i\gamma^{\mu}\partial_{\mu} - M_{\chi} + yh\right]\chi + \frac{1}{2}\partial_{\mu}h\partial^{\mu}h$$
$$-\frac{1}{2}M_h^2h^2 + f\frac{M_{\rm nucl.}}{v}\bar{\psi}h\psi. \quad (5)$$

In this model, χ and ψ represent the wave functions of the Dark Matter (DM) particle and nucleons, respectively. The interaction between the Higgs boson and nucleons follows a Yukawa-type coupling, characterized by the coupling constant f, which corresponds to the proton-Higgs form factor. We assume the Neutralino as the DM particle with a mass M_{χ} of 200 GeV. The parameters y and f are chosen as 0.07 and 0.35, respectively, based on constraints derived from experimental and empirical data. Additionally, the mass of the Higgs boson (M_h) is fixed at 125 GeV, while its vacuum expectation value (v) is set to 246 GeV.

Using the mean-field approximation the energy density and pressure for the DM can be expressed as [22, 26, 27, 28, 62, 63, 64],

$$\mathcal{E}_{\rm DM} = \frac{2}{(2\pi)^3}\int_0^{k_f^{\rm DM}} d^3k\sqrt{k^2 + (M_{\chi}^{\star})^2} + \frac{1}{2}M_h^2h_0^2, \quad (6)$$

and

$$P_{\rm DM} = \frac{2}{3(2\pi)^3}\int_0^{k_f^{\rm DM}} \frac{d^3k k^2}{\sqrt{k^2 + (M_{\chi}^{\star})^2}} - \frac{1}{2}M_h^2h_0^2, \quad (7)$$

where $k_f^{\rm DM}$ is the DM Fermi momentum.

2.3. The Complete Model for Dark Matter-admixed Quarkyonic Neutron Star

The total energy density and pressure of a DM-admixed quarkyonic star are then given by:

$$\mathcal{E} = \mathcal{E}_{\rm BM} + \mathcal{E}_{\rm QM} + \mathcal{E}_{\rm DM}, \quad (8)$$

and

$$P = P_{\rm BM} + P_{\rm QM} + P_{\rm DM}. \quad (9)$$

Here, $\mathcal{E}_{\rm BM}$, $\mathcal{E}_{\rm QM}$, and $\mathcal{E}_{\rm DM}$ denote the energy densities of baryonic matter, quark matter, and dark matter, respectively, while $P_{\rm BM}$, $P_{\rm QM}$, and $P_{\rm DM}$ represent their corresponding pressures. These quantities are derived from their respective Lagrangians and combined to obtain the total energy density $\mathcal{E}$ and pressure P, which are then utilized in the TOV equations to determine neutron star properties. The sharp phase transitions between quark and nucleonic matter often introduce discontinuities in the equation of state (EOS), which are smoothed out using Gibbs' criteria. The complete methodology is detailed in our previous works [3, 65].

2.4 Mass and Radius of the NS

We determine neutron star (NS) observables such as M and R by solving the Tolman-Oppenheimer-Volkoff (TOV) equations. For this, the equations of state (EOSs) of NSs incorporating dark matter (DM) are utilized as inputs to the TOV equations [66, 67, 3], which are expressed as:

$$\frac{dP_{tot.}(r)}{dr} = -\frac{(P_{tot.}(r) + \mathcal{E}_{tot.}(r))(m(r) + 4\pi r^3 P_{tot.}(r))}{r(r-2m(r))}, \quad (10)$$

and

$$\frac{dm(r)}{dr} = 4\pi r^2 \mathcal{E}_{tot.}(r). \quad (11)$$

Here, and $\mathcal{E}_{tot.}(r)$, $P_{tot.}(r)$ represent the total energy density and pressure, respectively, as functions of the radial distance r. The term $m(r)$ corresponds to the gravitational mass enclosed within a radius r. These coupled equations are solved simultaneously to determine the mass and radius of the neutron star for a given central density. Furthermore, in the study of neutron stars (NS) and general relativity, four types of curvature are used to describe the structure of space-time both inside and outside of stars. These four curvature measures are the Ricci scalar ($\mathcal{R}$), Ricci tensor ($\mathcal{J}$), Kretschmann scalar ($\mathcal{K}$), and Weyl tensor ($\mathcal{W}$). The details of the corresponding mathematical expression can be found in Refs. [37, 35, 29] and also in Appendix A.

3. Results and Discussions

This section explores the impact of various exotic components within a neutron star, studied through different types of spacetime curvatures. In our earlier work [3], we introduced the quarkyonic framework defined by two key parameters: the transition density (n_t) and the QCD confinement scale (Λ_{cs}). The parameter n_t determines the onset of quark formation, while Λ_{cs} acts as a momentum-scale cutoff distinguishing nucleons from quarks. Furthermore, the quarkyonic star model is extended to include the influence of dark matter (DM) by varying the DM Fermi momentum (k_f^{DM}), enabling a thorough investigation of its effects.

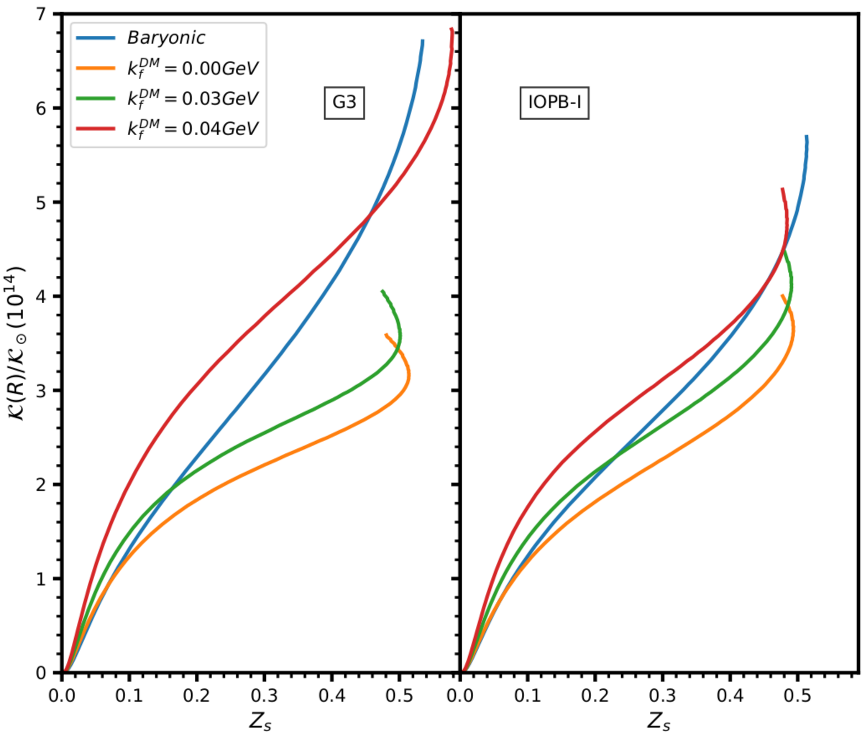

Figure1: The ratio of the Kretschmann scalar surface curvature of NS and the Sun $\mathcal{K}(R)/\mathcal{K}_\odot$ with the gravitational redshift at different transition densities, such as $n_t = 0.3, 0.4, 0.5 \mathrm{fm}^{-3}$, keeping the DM Fermi momentum k_f^{DM} and confinement scale parameter (Λ_{cs}) at 0.00 GeV and 800 MeV respectively for G3 and IOPB-I sets.

In Fig. 1, we have computed the variation of $\mathcal{K}(R)/\mathcal{K}_{\odot}$ with the gravitational redshift, where the Sun's surface curvature ($\mathcal{K}_{\odot}$) is 3.06 × 10 $^{-27}$ cm^{-2} . We noticed that the curvature ratio increases with Z_s for all cases, with DM-admixed stars exhibiting higher ratios compared to baryonic stars, indicating the significant role of DM in enhancing spacetime curvature. Higher DM Fermi momenta (k_f^{DM} = 0.03, 0.04 GeV) result in progressively larger curvature ratios, reflecting the stiffening effect of DM on the quarkyonic EOS. The G3 force produces consistently higher curvature values than IOPB-I. The relative differences between baryonic and DM-admixed curves are more pronounced for G3 than IOPB-I, reflecting variations in the interplay of quarkyonic matter stiffness and DM softening between the two forces. Gravitational redshift, as a probe of compactness, effectively captures the impact of DM admixture on neutron star curvature properties.

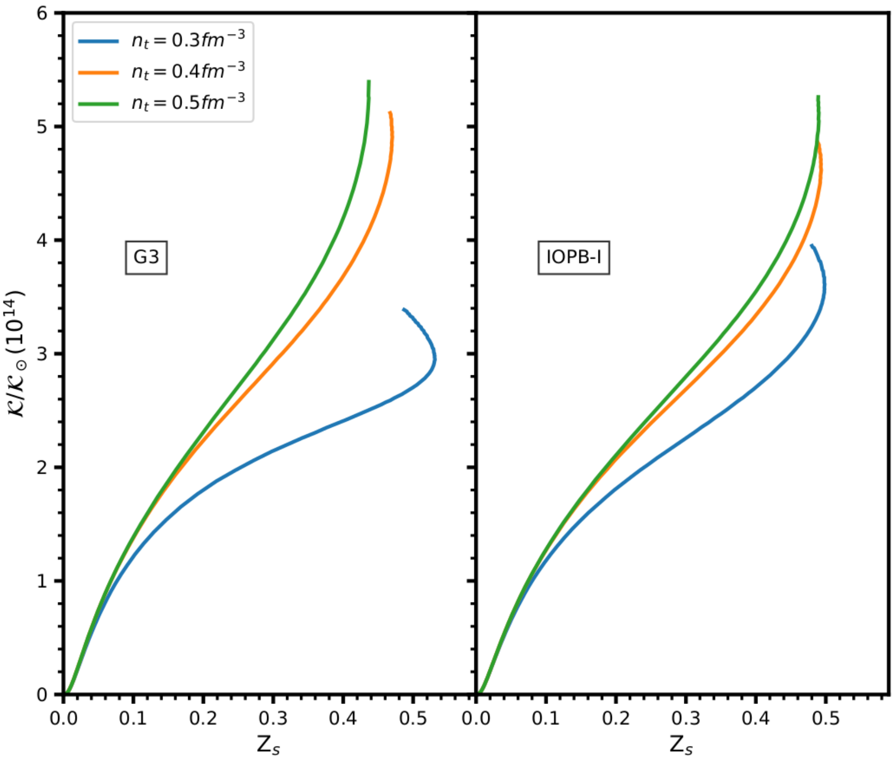

Figure 2: The ratio of the Kretschmann scalar surface curvature of NS and the Sun $\mathcal{K}(R)/\mathcal{K}_{\odot}$ with the gravitational redshift at different transition

densities, such as $n_t = 0.3, 0.4, 0.5 \mathrm{fm}^{-3}$, keeping the DM Fermi momentum k_f^{DM} and confinement scale parameter (Λ_{cs}) at 0.00 GeV and 800 MeV respectively for G3 and IOPB-I sets.

Further, we have extended our analysis, by varying the transition densities, such as n_t = 0.3, 0.4, 0.5 fm^{-3} as they are crucial in the formation of a quarkyonic core. In Fig. 2, the same is presented as in Fig.2, but with the change in transition densities. From the analysis, it is noticed that for G3 set, at n_t = 0.3 fm^{-3}, the curvature ratio consistently rises with increasing gravitational redshift, maintaining a steeper slope than higher transition densities. At n_t= 0.4 fm^{-3}, the slope decreases slightly, reflecting a lower value of surface curvature. At n_t = 0.5 fm^{-3}, the ratio grows more gradually, indicating a softer EOS effect at higher transition densities. For IOPB-I EOS, Similar trends are observed, but the absolute values of the ratio are generally lower compared to G3. Moreover, The dependence of surface curvature on transition density (n_t) emphasizes the sensitivity of NS properties to the EOS parameters.

4. Conclusions

In conclusion, we carried out a comprehensive analysis of the curvature properties of quarkyonic stars, focusing on the impact of dark matter within the effective relativistic mean-field (E-RMF) framework. The study examined gravitational curvature quantity such as the Kretschmann scalar (K) which offers valuable insights into the strong-field regime of general relativity and the internal structure of neutron stars. The calculations utilized two well-established nuclear parameter sets, G3 and IOPB-I, which are characterized by their differing stiffness in modeling the equation of state (EOS) for dense nuclear matter. The presence of DM within neutron stars significantly enhances their spacetime curvature. This is evident from the ratio of the Kretschmann scalar surface curvature of the neutron star to that of the Sun $(\mathcal{K}(\mathcal{R})/\mathcal{K}_{\odot})$. Stars with higher DM Fermi momenta (k_f^{DM} = 0.03, 0.04 GeV) exhibit larger curvature ratios compared to purely baryonic stars. This enhancement reflects the stiffening effect of DM on the quarkyonic equation of state (EOS). Gravitational redshift, as a measure of compactness, effectively captures these variations, showcasing the interplay between DM and spacetime curvature. Furthermore, the choice of nuclear force also influences the curvature properties. The G3 (soft) force produces consistently higher curvature values than the IOPB-I (stiff) force. Again, the transition density (n_t) plays a critical role in shaping neutron star curvature. Lower transition densities (n_t= 0.3 fm^{-3}) lead to steeper increases in the curvature ratio with gravitational redshift, reflecting a stiffer EOS and a more compact structure.

Appendix A: Mathematical expressions for various curvatures

In the study of neutron stars (NS) and general relativity, four types of curvature are used to describe the structure of space-time both inside and outside of stars. These four curvature measures are the Ricci scalar ($\mathcal{R}$), Ricci tensor ($\mathcal{J}$), Kretschmann scalar ($\mathcal{K}$), and Weyl tensor ($\mathcal{W}$). The corresponding mathematical expressions are given as follows, the Ricci scalar,

$$\mathcal{R}(r) = 8\pi\left[\mathcal{E}_{tot.}(r) - 3P_{tot.}(r)\right], \quad (1)$$

the square root of the full contraction of the Ricci tensor is defined as

$$\mathcal{J}(r) \equiv \sqrt{\mathcal{R}_{\mu\nu}\mathcal{R}^{\mu\nu}} = \left[(8\pi)^2\left[\mathcal{E}^2_{tot.}(r) + 3P^2_{tot.}(r)\right]\right]^{1/2}, \quad (2)$$

the Kretschmann scalar is defined as the square root of the full contraction of the Riemann tensor.

$$\begin{aligned}\mathcal{K}(r) &\equiv \sqrt{\mathcal{R}^{\mu\nu\rho\sigma}\mathcal{R}_{\mu\nu\rho\sigma}} \\ &= \Bigg[(8\pi)^2[3\mathcal{E}^2_{tot.}(r) + 3P^2_{tot.}(r) + 2P_{tot.}(r)\mathcal{E}_{tot.}(r)] \\ &\quad - \frac{128\mathcal{E}_{tot.}(r)m(r)}{r^3} + \frac{48m^2(r)}{r^6}\Bigg]^{1/2}, \quad (3)\end{aligned}$$

and the square root of the full contraction of the Weyl tensor

$$\mathcal{W}(r) \equiv \sqrt{\mathcal{C}^{\mu\nu\rho\sigma}\mathcal{C}_{\mu\nu\rho\sigma}} = \left[\frac{4}{3}\left(\frac{6m(r)}{r^3} - 8\pi\mathcal{E}_{tot.}(r)\right)^2\right]^{1/2}. \quad (4)$$

Here $\mathcal{E}_{tot.}$, $P_{tot.}$, $m(r)$ are the energy density, pressure, and mass of the NS as a function of radius respectively. The $\mathbb{K}$ and $\mathbb{W}$ curvature are present inside and outside of the star i.e. in a vacuum. Contrary to this $\mathbb{R}$ and $\mathbb{J}$ are only confined within the star. More details can be found in Refs. [37, 35, 29].

References

[1] S. Shapiro and S. Teukolsky, Black holes, white dwarfs, and neutron stars: The physics of compact objects (John Wiley & Sons, Ltd, 1983).

[2] J. M. Lattimer and M. Prakash, Phys. Reports 442, 109 (2007), the Hans Bethe Centennial Volume 1906-2006.

[3] D. Dey, J. A. Pattnaik, H. C. Das, A. Kumar, R. N. Panda, and S. K. Patra, Dark matter influence on quarkyonic stars: A relativistic mean field analysis (2024), arXiv:2401.02190 [astroph.HE, (Accepted in JCAP)].

[4] B. P. Abbott, R. Abbott, T. D. Abbott, et al. (LIGO Scientific Collaboration and Virgo Collaboration), Phys. Rev. Lett. 119, 161101 (2017).

[5] S. De, D. Finstad, J. M. Lattimer, D. A. Brown, E. Berger, and C. M. Biwer, Phys. Rev. Lett. 121, 091102 (2018).

[6] B. P. Abbott, R. Abbott, T. D. Abbott, et al. (The LIGO Scientific Collaboration and the Virgo Collaboration), Phys. Rev. Lett. 121, 161101(2018).

[7] C. D. Capano, I. Tews, S. M. Brown, B. Margalit, S. De, S. Kumar, D. A. Brown, B. Krishnan, and S. Reddy, Nature Astronomy 4, 625 (2020).

[8] T. E. Riley, A. L. Watts, S. Bogdanov, et al., APJL 887, L21 (2019).

[9] M. C. Miller, F. K. Lamb, A. J. Dittmann, and other, The Astrophysical Journal Letters 887, L24 (2019).

[10] J. M. Lattimer, Annual Review of Nuclear and Particle Science 62, 485 (2012).

[11] F. Ozel and P. Freire, araa 54, 401 (2016), arXiv:1603.02698.

[12] R. W. Romani, D. Kandel, A. V. Filippenko, T. G. Brink, and W. Zheng, The Astrophysical Journal Letters 934, L17 (2022).

[13] H. T. Cromartie, E. Fonseca, S. M. Ransom, P. B. Demorest, Z. Arzoumanian, et al., Nature Astronomy 4, 72–76 (2020).

[14] T. Zhao and J. M. Lattimer, Phys. Rev. D 102, 023021 (2020).

[15] R. Abbott, T. D. Abbott, S. Abraham, F. Acernese, K. Ackley, C. Adams, R. X. Adhikari, V. B. Adya, C. Affeldt, M. Agathos, and all, The Astrophysical Journal Letters 896, L44 (2020).

[16] F. Sandin and P. Ciarcelluti, Astroparticle Phys. 32, 278–284 (2009).

[17] A. De Lavallaz and M. Fairbairn, Phys. Rev. D 81, 123521 (2010).

[18] C. Kouvaris and P. Tinyakov, Phys. Rev. D 82, 063531 (2010).

[19] P. Ciarcelluti and F. Sandin, Phys. Lett. B 695, 19–21 (2011).

[20] S.-C. Leung, M.-C. Chu, and L.-M. Lin, Phys. Rev. D 84, 107301 (2011).

[21] A. Li, F. Huang, and R.-X. Xu, Astroparticle Phys. 37, 70–74 (2012).
[22] G. Panotopoulos and I. Lopes, Phys. Rev. D 96, 083004 (2017).
[23] J. Ellis, G. Hutsi, K. Kannike, ¨ et al., Phys. Rev. D 97, 123007 (2018).
[24] S. A. Bhat and A. Paul, The European Physical Journal C 80, 544 (2020).
[25] O. Ivanytskyi, V. Sagun, and I. Lopes, Neutron stars: new constraints on asymmetric dark matter (2019), arXiv:1910.09925 [astro-ph.HE].
[26] A. Das, T. Malik, and A. C. Nayak, Phys. Rev. D 99, 043016 (2019).
[27] A. Quddus, G. Panotopoulos, B. Kumar, S. Ahmad, and S. K. Patra, Journal of Physics G: Nuclear and Particle Physics 47, 095202 (2020).
[28] H. C. Das, A. Kumar, B. Kumar, S. K. Biswal, T. Nakatsukasa, A. Li, and S. K. Patra, Monthly Notices of the Royal Astronomical Society 495, 4893 (2020).
[29] H. Das, A. Kumar, B. Kumar, S. Biswal, and S. Patra, Journal of Cosmology and Astroparticle Physics 2021 (01), 007.
[30] B. Kumar, S. Singh, B. Agrawal, and S. Patra, Nuclear Physics A 966, 197 (2017).
[31] B. Kumar, S. K. Patra, and B. K. Agrawal, Phys. Rev. C 97, 045806 (2018).
[32] J. A. Pattnaik, M. Bhuyan, R. N. Panda, and S. K. Patra, Physica Scripta 96, 125319 (2021).
[33] J. A. Pattnaik, R. N. Panda, M. Bhuyan, and S. K. Patra, Chinese Physics C 46, 094103 (2022).
[34] D. Psaltis, Living Rev. Relativity. 11, 9 (2008).
[35] X.-T. He, F. J. Fattoyev, B.-A. Li, and W. G. Newton, Phys. Rev. C 91, 015810 (2015).
[36] S. M. Carroll, Spacetime and Geometry: An Introduction to General Relativit(Cambridge University Press, 2019).
[37] K. Y. Eksi, C. Gungor, and M. M. Turkoglu, Phys. Rev. D 89, 063003 (2014).
[38] H. C. Das, J. A. Pattnaik, and S. K. Patra, Phys. Rev. D 107, 083007 (2023).
[39] J. A. Pattnaik, J. T. Majekodunmi, A. Kumar, M. Bhuyan, and S. K. Patra, Phys. Rev. C 105, 014318 (2022).
[40] J. A. Pattnaik, K. C. Naik, R. N. Panda, M. Bhuyan, and S. K. Patra, Pramana 97, 136 (2023).
[41] G. A. Lalazissis, J. Konig, and P. Ring, Phys. Rev. C 55, 540 (1997).
[42] M. Rashdan, Phys. Rev. C 63, 044303 (2001).
[43] A. Sulaksono and T. Mart, Phys. Rev. C 74, 045806 (2006).
[44] D. P. Menezes and C. Providencia, Phys. Rev. C 70, 058801 (2004).

[45] G. Lalazissis, S. Karatzikos, R. Fossion, D. P. Arteaga, A. Afanasjev, and P. Ring, Physics Letters B 671, 36 (2009).
[46] F. J. Fattoyev, C. J. Horowitz, J. Piekarewicz, and G. Shen, Phys. Rev. C 82, 055803 (2010).
[47] A. b. A. Dadi, Phys. Rev. C 82, 025203 (2010).
[48] X. Roca-Maza, X. Vinas, M. Centelles, P. Ring, and P. Schuck, ˜ Phys. Rev. C 84, 054309 (2011).
[49] B.-J. Cai and L.-W. Chen, Phys. Rev. C 85, 024302 (2012).
[50] F. J. Fattoyev, C. J. Horowitz, J. Piekarewicz, and B. Reed, Phys. Rev. C 102, 065805 (2020).
[51] S. K. Patra, M. Centelles, X. Vinas, and M. Del Estal, Phys. Rev. C 65, 044304 (2002).
[52] H. Muller and B. D. Serot, Nuclear Physics A 606, 508 (1996).
[53] P. Wang, Phys. Rev. C 61, 054904 (2000).
[54] A. Kumar, H. C. Das, S. K. Biswal, B. Kumar, and S. K. Patra, The European Physical Journal C 80, 775 (2020).
[55] L. D. Miller and A. E. S. Green, Phys. Rev. C 5, 241 (1972).
[56] B. D. Serot and J. D. Walecka, Relativistic nuclear many-body theory, in Recent Progress in Many-Body Theories: Volume 3, edited by T. L. Ainsworth, C. E. Campbell, B. E. Clements, and E. Krotscheck (Springer US, Boston, MA, 1992) pp. 49–92.
[57] R. J. Furnstahl, C. E. Price, and G. E. Walker, Phys. Rev. C 36, 2590 (1987).
[58] P.-G. Reinhard, Zeitschrift fur Physik A Atomic Nuclei 329, 257 (1988).
[59] R. Furnstahl, B. D. Serot, and H.-B. Tang, Nuclear Physics A 615, 441 (1997).
[60] L. McLerran and S. Reddy, Phys. Rev. Lett. 122, 122701 (2019).
[61] J. M. Cline, P. Scott, K. Kainulainen, and C. Weniger, Phys. Rev. D 88, 055025 (2013).
[62] H. C. Das, A. Kumar, and S. K. Patra, Monthly Notices of the Royal Astronomical Society 507, 4053 (2021).
[63] H. C. Das, A. Kumar, B. Kumar, and S. K. Patra, Galaxies 10, 10.3390/galaxies10010014 (2022).
[64] H. C. Das, A. Kumar, S. K. Biswal, and S. K. Patra, Phys. Rev. D 104, 123006 (2021).
[65] B. K. Sharma, P. K. Panda, and S. K. Patra, Phys. Rev. C 75, 035808 (2007).
[66] R. C. Tolman, Phys. Rev. 55, 364 (1939).
[67] J. R. Oppenheimer and G. M. Volkoff, Phys. Rev. 55, 374 (1939).